Optical properties of Ga-doped AlN nanowires

Rémy Vermeersch, Gwénolé Jacopin, Eric Robin, Julien Pernot, Bruno Gayral, Bruno Daudin

Optical properties of Ga-doped AlN nanowires

Rémy Vermeersch[1,2], Gwénolé Jacopin[1], Eric Robin[3], Julien Pernot[1], Bruno Gayral[2], Bruno Daudin[2]

[1] Univ. Grenoble Alpes, Grenoble INP, Institut Néel, CNRS, 38000 Grenoble, France.

[2] Univ. Grenoble Alpes, Grenoble INP, CEA, IRIG-PHELIQS, NPSC, 17 rue des martyrs, 38000 Grenoble, France.

[3] Univ. Grenoble Alpes, Grenoble INP, CEA, IRIG-MEM, LEMMA, 17 rue des martyrs, 38000 Grenoble, France.

Corresponding author: remy.vermeersch@neel.cnrs.fr ; bruno.daudin@cea.fr

Abstract

We show that the intentional Ga doping of AlN nanowires in the 0.01-0.5 percent range leads to the spontaneous formation of nanometric carrier localization centers. Accordingly, for single nanowires, we observed a collection of sharp cathodoluminescence lines in a wavelength range spanning from 220 to 300 nm. From temperature dependent cathodoluminescence a ratio between the intensity at room temperature and 5 K of 20-30 % is measured. We found that an ensemble of Ga-doped AlN nanowires exhibits a wide-band cathodoluminescence emission, which opens the path to the realization of efficient UV-C light emitting diodes covering a wide part of DNA absorption band.

The direct band gap of GaN (3.5 eV, 350 nm) and AlN (6.2 eV, 205 nm) and the expected full miscibility of these two compounds[1] potentially makes AlGaN heterostructures particularly interesting for UV-emitting opto-electronic devices. However, despite such a full miscibility range, the optical properties of AlGaN alloy layers are generally affected by composition fluctuations related to the different Ga and Al diffusion length on the growing surface[2] and to the presence of extended defects such as dislocations[3] or grain boundaries.[4] In the case of AlGaN nanowires (NWs), which are free of extended defects and subject for this reason to a growing interest, the spontaneous formation of alternated Al- and Ga-rich layers was observed by several groups and can be assigned to the specificities of the NW growth mode.[5,6] Besides such extrinsic alloy composition fluctuations, intrinsic alloy disorder is deeply affecting the optical properties of AlGaN alloys, due to both the small exciton Bohr radius[7] and the large difference in band gap values of the two binaries.[8] The tiny volume of single NWs is particularly favorable to the observation of individual localization centers resulting from such alloy composition fluctuations. In particular, photoluminescence (PL) spectra of single AlGaN NWs have revealed the presence of a wide distribution of sharp lines exhibiting a quantum dot behavior, assigned to a large diversity of local Al-Ga-N configurations at the nanoscale.[5] The large values of exciton and carrier localization energies in the Al-Ga-N ternary system are expected to favor radiative recombination efficiency in related opto-electronic devices. Along these lines, it is the purpose of the present study to examine the case of Ga-doped AlN NWs in the limit of very low Ga content, typically below 0.5%. It will be shown that short range alloy composition fluctuations are leading to the formation of a collection of carrier localization centers spanning on a wide energy scale. Furthermore, it will be demonstrated that these localization centers behave as carrier-confining quantum dots and may provide a path for the elaboration of efficient UV-emitting light sources exhibiting large radiative recombination efficiency.

The samples were grown by plasma-assisted molecular beam epitaxy (PA-MBE) on a (111) Si substrate. Following the deposition of a pseudo template formed of GaN NWs spontaneously nucleated on Si, a Ga-doped AlN NW section was further grown using an Al/N flux ratio equal to 0.56 and a growth temperature of 750°C. The typical AlN NW diameter was in the 50 -90 nm range, small enough to promote a pure elastic strain relaxation of the AlN section grown on the GaN stem and no extended defect formation.[9] Four different Ga fluxes were used corresponding to Ga cell temperatures of 770, 790, 810 and 840 °C, further denominated Ga770, Ga790, Ga810 and Ga840, respectively. An additional sample was grown

in the same conditions without any Ga flux during the AlN growth to be used as a reference. The scheme of the samples and the scanning electron microscopy (SEM) image of sample Ga790 are shown in figure 1a and 1b, respectively.

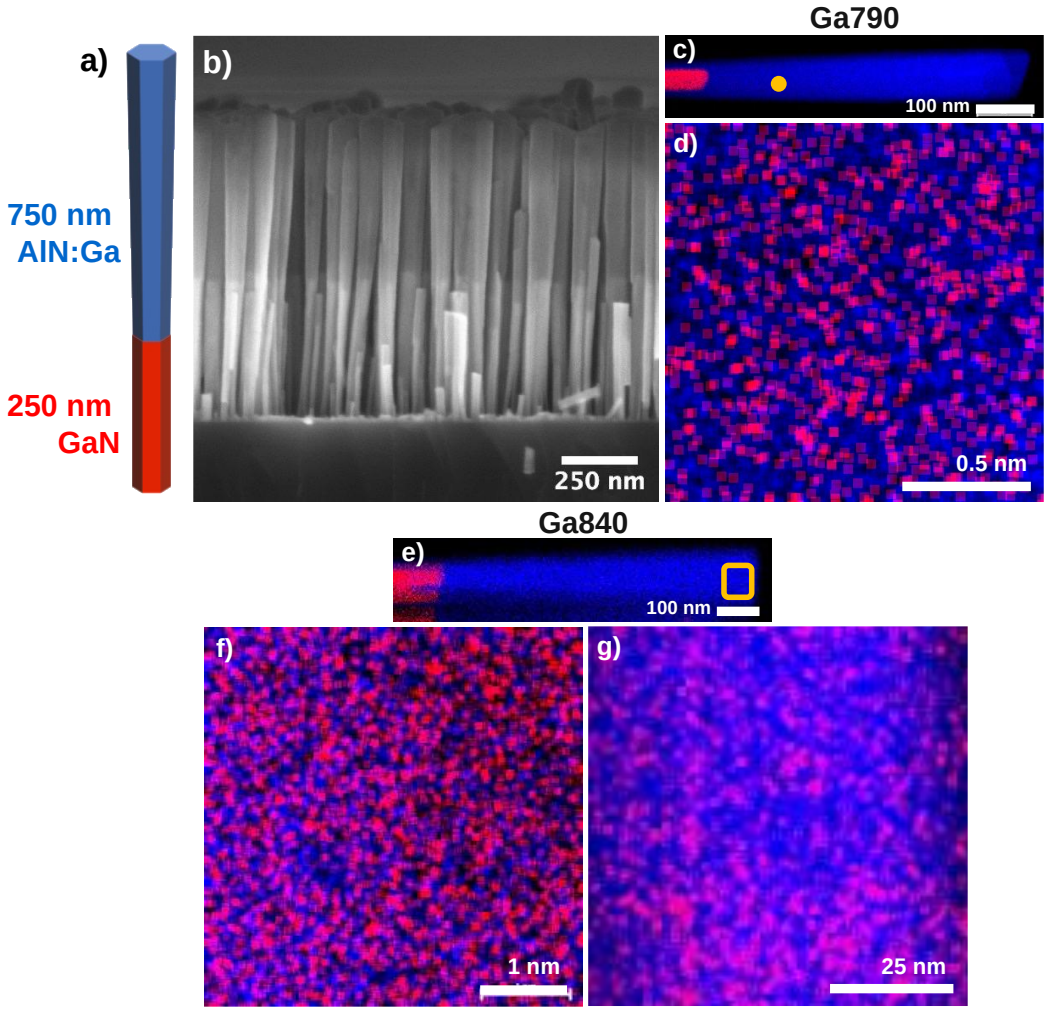

Figure 1: (a) scheme of the samples. (b) SEM image of NWs in sample Ga790. (c)&(e) Ga (red) and Al (blue) EDX mapping of a single NW of Ga790 and Ga840. (d) zoomed Ga and Al EDX mapping corresponding to the spot in (c). (f)-(g) zoomed Ga and Al EDX mapping corresponding to the rectangle (e), at the upper end of a single NW of sample Ga840.

The Ga content in the AlN sections of the heterostructure was determined by energy dispersive x-rays (EDX) spectroscopy. For this purpose, high resolution scanning transmission electron microscopy (HR-STEM) images of single NWs were acquired in high angle annular dark field (HAADF) mode and energy dispersive X-ray spectroscopy (EDX) was performed on a probe-corrected FEI Titan Themis equipped with four windowless silicon drift detectors. X-

ray spectra were acquired at 200 keV with high current probe. The net intensities of N K-line (Kα: 0.39 keV), Al K- lines (Kα: 1.49 keV; Kβ: 1.56 keV), and Ga K-lines (Kα: 9.23−9.25 keV; Kβ: 10.26−10.35 keV) were extracted from the X-ray spectra using the QUANTAX-800 software from Bruker. The conversion of the net X-ray intensities into concentrations was performed using the zeta-factor method allowing one to correct intensities from X-ray absorption.[10]

The Ga and Al elemental mapping of single dispersed NWs from samples Ga790 and Ga840 are shown in figure 1c-g. (Raw EDX spectra are available in the supplementary materials section A). For both samples, the average Ga content was extracted from figure 1c and 1e and found to be in the range 0.05 ± 0.05 to 0.11 ± 0.01 %, close to the EDX detection limit and markedly lower than the expected nominal composition, which is assigned to the large difference in sticking coefficient/incorporation rate of Ga and Al for the growth temperature used.[11] As shown in figure 1d, 1f and 1g, strong Ga content fluctuations were locally put in evidence at different scale, with a local Ga content up to 0.4 %. However, it is worth stressing that Ga mapping is indeed a planar projection along the 100 nm diameter of dispersed NWs, so that the presence of composition fluctuations smaller in size cannot be excluded. More generally, the average Ga content and the size of the composition fluctuations under scrutiny are directly related with the volume probed by EDX, itself depending on experimental conditions and NW morphology.

In order to probe the optical properties of the studied samples, cathodoluminescence (CL) experiments have been carried out in a custom FEI Inspect F50 scanning SEM. The signal was detected through a Horiba Jobin Yvon iHR 550 spectrometer equipped with 1800 grooves.mm^{-1} gratings (0.013 nm/pixel) and a Peltier-cooled Andor Technology Newton DU940 CCD. The beam size was of around 20 nm in diameter and an acceleration voltage of 15 kV was applied corresponding to an interaction region depth of ~1µm. Top–view CL results shown in figure 2a exhibit a wide band emission for all four Ga-doped AlN samples, extending from about 220 to 300 nm. As the Ga flux decreases, an additional peak is found to shift toward smaller wavelengths, along with a decrease in the low energy peak intensity. Regarding the luminescence of the un-doped reference sample, a single band centered at 245 nm is measured, away from the trend observed for the Ga containing samples. Remarkably, sharp lines are put in evidence when probing a reduced number of NWs (figure 2b), suggesting the presence of a wide distribution of carrier localization centers dominating the luminescence properties of single NWs. In figure 2b, the black line corresponds to the CL spectrum averaged on eight

different spots, which is similar to the ensemble CL spectrum for Ga790 shown in figure 2a. Additional photoluminescence experiments were performed on sample Ga840 using a continuous-wave frequency-doubled beam at 244 nm (see supplementary materials, section B). The focused spot size was of 40 µm in diameter. No shape change of the emission band was observed in an excitation range from 5 to 480 µW, as a first clue that the wide band emission does not result from the presence of donor-acceptor pairs (DAP) although this statement has to be balanced by the weak absorption at 244 nm in the sample. In contrast, the same experiment was performed on the reference sample and CL revealed no sharp lines. In addition, a decrease in PL intensity when increasing the excitation power is observed in this reference sample. This behavior, typical of the saturation of defect-related emission for increasing excitation power, is consistent with the presence of unidentified point defects as main luminescence centers in this sample and tentatively assigned to oxygen impurities. [12,13]

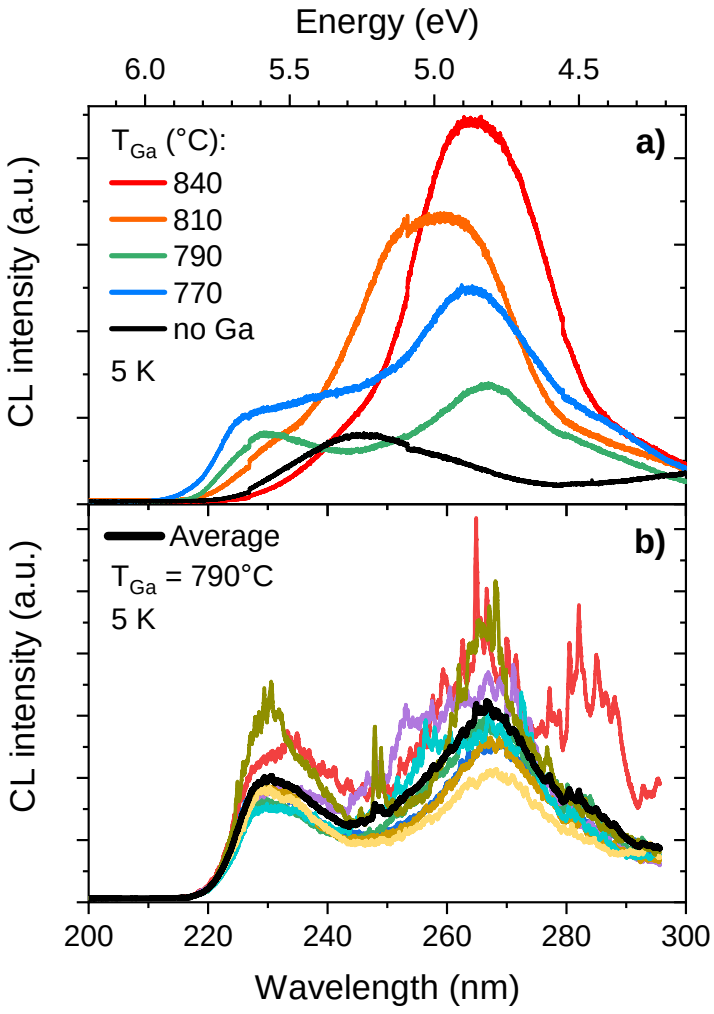

Figure 2: (a) 100 µm² field CL spectra at 5K of the 5 different samples. (b) CL spots recorded at 5K on Ga790, putting in evidence sharp lines randomly distributed. The black line corresponds to the averaged CL on eight different spots.

In order to shed light on the spatial distribution of carrier localization centers along the growth axis, low temperature CL experiments were also performed on single dispersed NWs, in the same configuration. Results for one NW of sample Ga790 are shown in figure 3a, assessing a random distribution of single emission peaks along the growth axis. The full width at half maximum (FWHM) of isolated single lines was in the 1 - 5 meV range. Time resolved CL measurements allowed us to extract a decay time in the 0.2 - 0.4 ns range (more details in the supplementary materials section C). These two observations are consistent with the values reported by Belloeil et al. in the case of single carrier localization centers assigned to composition fluctuations in AlGaN NWs.[14] As shown in figure 3c, no single emission peaks are observed in the reference sample, as a further confirmation that CL emission in this sample is not related to Ga doping.

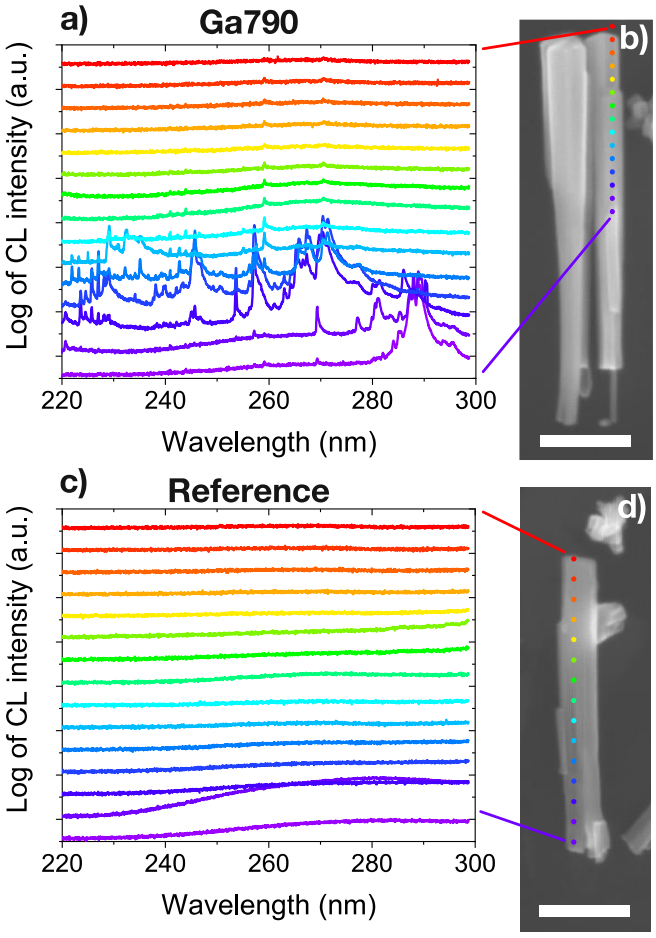

Figure 3: (a) Low temperature CL spectra at different spots along the growth axis of a single NW of (b) sample Ga790. (c) Low temperature CL spectra at different spots along the growth axis of a single NW of (d) the reference sample. CL spectra are plotted in log scale. The scale bars in (b) and (d) are 250 nm.

The variation of CL intensity as a function of temperature is plotted in figure 4 for Ga790 and Ga840. The integrated intensity variation as a function of temperature plotted in inset shows that at room temperature it is still 20-30% of the low temperature intensity value. Consistent with the EDX results, we assign this limited quenching to the quantum dot-like behavior of the carrier localization centers resulting from the local Ga concentration fluctuations. The marked variability of the CL spectra from one NW to another or from one spot to another inferred from the results plotted in figure 2b further suggests a random distribution of a variety of carrier localization centers from NW to NW, depending on the local chemical configuration.

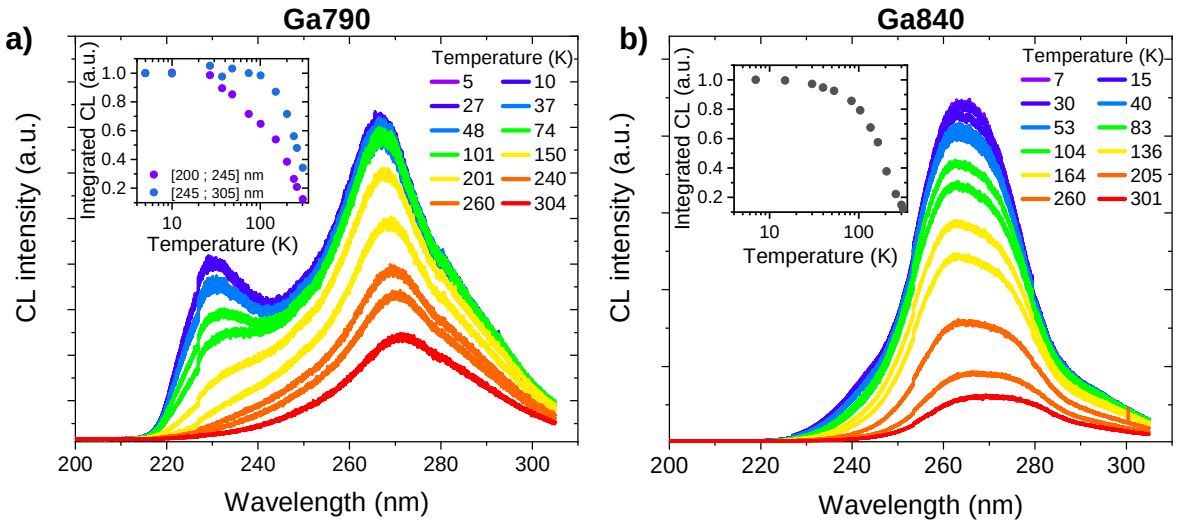

Figure 4: (a) CL spectra of Ga790 between 5K and 300K. The dotted lines are pointing the CL peak maximum. Inset: integrated CL intensity as a function of temperature for [200-245] nm and [245-305] nm wavelength windows. (b) The same for Ga840. Inset: integrated CL intensity as a function of temperature.

Interestingly, in figure 4a, the quenching of the low wavelength peak is far more important than for its longer wavelength counterpart. As the shape of the CL peaks is directly correlated to the Ga content and exhibits growth-temperature related modifications when changing the analysis spot along the wafer diameter, we discard the possibility that the low wavelength contribution could be associated with another kind of point defects in Ga790. In particular, the CL signature observed in the 220 - 240 nm wavelength range in the reference sample (figure 3c) does not overlap the low wavelength contribution in Ga790, ruling out the possibility of a common origin of both CL signatures. Accordingly, the temperature stability of the long wavelength CL peak up to 100K in Ga790 rather suggests a carrier transfer from one

population of carrier localization centers to the other. This assumption is supported by the behavior observed for Ga840 in figure 4b where the low wavelength wing of the wide CL band is indeed decreasing faster as a function of temperature than on the long wavelength side, also pointing out in this case towards a carrier transfer from high energy emitting localization centers to low energy emitting ones.

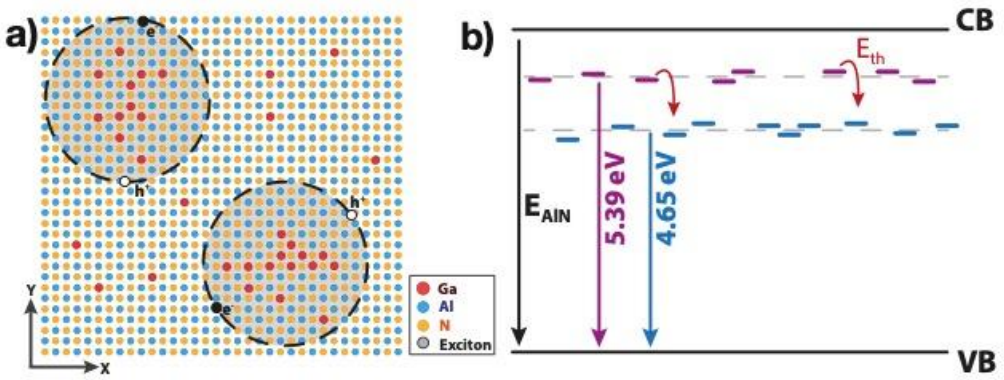

Figure 5: (a) schematics of Al and Ga composition fluctuations at the scale of the exciton in AlN. (b) schematics of the band structure showing the distribution of two populations of deep state levels assigned to local Ga composition fluctuations. E_{th} stands for thermal energy.

Figure 5a shows a schematic view of local composition fluctuations in Ga-doped AlN, leading to the formation of localization centres deep in the gap, as proposed in figure 5b. Contrary to the case of low localization energy value, usually characterized by a so-called S-shaped curve when plotting the emission peak energy as a function of temperature, no S-shaped curve is observed in the present case. This is attributed to the large localization energy related to Ga local environment fluctuations, which suggests that carrier localization is still dominating at room temperature, consistent with the limited quenching of CL intensity between low and room temperature and further supporting a carrier transfer from one localization energy distribution to the other.

Recently, nano-emitter formation was reported in N-doped GaAs[15] and GaAsP[16] NWs for N content lower than 1%. Similar to the present case, a collection of sharp optical emission lines was observed, which was assigned to local N composition fluctuations, the wide energy distribution of these emitters resulting from various degrees of N clustering correlated to the anomalous band gap bowing in GaAsN.[17] Such an explanation is hardly to be at play in the present case of the AlGaN system which exhibits a small band gap bowing. However, due to the small size of the exciton Bohr radius in AlN, namely 1.9 nm[7], local fluctuations involving

a limited number of Ga atoms and/or the formation of Ga nano-clusters kinetically driven on the growth front may be sufficient to drastically affect the recombination emission assigned to the formation of a collection of local atomic configurations at the sub-nanometer scale. However, the detailed formation mechanism of Ga-rich clusters is still unclear at this stage. In particular, CL observed around 270 nm in figure 4 implies local Ga concentration far higher than the average content, suggesting spontaneous Ga accumulation. Similarly to the well-known case of quantum dots vertical correlation[18,19], it suggests that the stochastic incorporation of single Ga atoms in the AlN matrix, could be followed by the energetically favorable incorporation of additional Ga atoms in the top layers in the close vicinity of the first Ga atom, which would lead to local Ga accumulation.

The wide band emission of Ga-doped AlN, overlapping a large part of DNA absorption band, potentially appears as well adapted to the realization of efficient deep UV LEDs compared to the sharp 253.6 nm emission line of low pressure Hg lamps[20]. Accordingly, the recent demonstration of n-type and p-type doping of AlN NWs[21–23] indeed opened the path to the realization of full AlN NWs UV-C LEDs containing a Ga-doped AlN active region with a Ga content which could be tuned according to the targeted wavelength emission.

In summary, we have investigated the structural and optical properties of Ga-doped AlN NWs, for an average Ga content below 0.5%. EDX experiments have provided the evidence for marked local Ga composition fluctuations at the nm scale, responsible for the formation of QD-like emitters. Accordingly, sharp emission lines were observed by CL along with evidence for a significant carrier confinement. The wide range of emission line energies, spanning from about 220 to 300 nm paves the way for the realization of a new class of efficient NW UV-C emitters with a Ga doped AlN active region. Such emitters indeed cover a wide part of DNA absorption band and could be suitable for disinfection applications.

Acknowledgments

The authors thank Y. Genuist, Y. Curé and F. Jourdan from CEA Grenoble for technical support during MBE growth and Dr. F. Donatini for his help with the CL setup. We acknowledge support from GANEXT (ANR-11-LABX-0014). GANEXT belongs to the public funded 'Investissements d'Avenir' program managed by the French ANR agency.

The authors declare no conflict of interests.

References

[1] I.H. Ho and G.B. Stringfellow, MRS Proc. **449**, 871 (1996).

[2] I. Bryan, Z. Bryan, S. Mita, A. Rice, L. Hussey, C. Shelton, J. Tweedie, J.-P. Maria, R. Collazo, and Z. Sitar, J. Cryst. Growth **451**, 65 (2016).

[3] L. Chang, S.K. Lai, F.R. Chen, and J.J. Kai, Appl. Phys. Lett. **79**, 928 (2001).

[4] A. Pinos, V. Liuolia, S. Marcinkevičius, J. Yang, R. Gaska, and M.S. Shur, J. Appl. Phys. **109**, 113516 (2011).

[5] A. Pierret, C. Bougerol, M. den Hertog, B. Gayral, M. Kociak, H. Renevier, and B. Daudin, Phys. Status Solidi - Rapid Res. Lett. **7**, 868 (2013).

[6] S. Zhao, S.Y. Woo, M. Bugnet, X. Liu, J. Kang, G.A. Botton, and Z. Mi, Nano Lett. **15**, 7801 (2015).

[7] T. Onuma, S.F. Chichibu, T. Sota, K. Asai, S. Sumiya, T. Shibata, and M. Tanaka, Appl. Phys. Lett. **81**, 652 (2002).

[8] N. Nepal, J. Li, M.L. Nakarmi, J.Y. Lin, and H.X. Jiang, Appl. Phys. Lett. **88**, 2005 (2006).

[9] F. Glas, Phys. Rev. B - Condens. Matter Mater. Phys. **74**, 2 (2006).

[10] E. Robin, N. Mollard, K. Guilloy, N. Pauc, P. Gentile, Z. Fang, B. Daudin, L. Amichi, P.-H. Jouneau, C. Bougerol, M. Delalande, and A.-L. Bavencove, in *Eur. Microsc. Congr. 2016 Proc.* (Wiley-VCH Verlag GmbH & Co. KGaA, Weinheim, Germany, 2016), pp. 380–381.

[11] E. Iliopoulos, K.F. Ludwig, T.D. Moustakas, P. Komninou, T. Karakostas, G. Nouet, and S.N.G. Chu, Mater. Sci. Eng. B Solid-State Mater. Adv. Technol. **87**, 227 (2001).

[12] C. Hartmann, L. Matiwe, J. Wollweber, I. Gamov, K. Irmscher, M. Bickermann, and T. Straubinger, CrystEngComm **22**, 1762 (2020).

[13] G.A. Slack, L.J. Schowalter, D. Morelli, and J.A. Freitas, J. Cryst. Growth **246**, 287 (2002).

[14] M. Belloeil, B. Gayral, and B. Daudin, Nano Lett. **16**, 960 (2016).

[15] S. Filippov, M. Jansson, J.E. Stehr, J. Palisaitis, P.O.A. Persson, F. Ishikawa, W.M. Chen, and I.A. Buyanova, Nanoscale **8**, 15939 (2016).

[16] M. Jansson, L. Francaviglia, R. La, C.W. Tu, W.M. Chen, and I.A. Buyanova, Phys. Rev. Mater. **4**, 1 (2020).

[17] U. Tisch, E. Finkman, and J. Salzman, Appl. Phys. Lett. **81**, 463 (2002).

[18] C. Adelmann, M. Arlery, B. Daudin, G. Feuillet, G. Fishman, L.S. Dang, H. Mariette, N. Pelekanos, J.-L. Rouvière, J. Simon, and F. Widmann, Comptes Rendus l'Académie Des Sci. - Ser. IV - Phys. **1**, 61 (2000).

[19] J. Coraux, H. Renevier, V. Favre-Nicolin, G. Renaud, and B. Daudin, Appl. Phys. Lett. **88**, 153125 (2006).

[20] K. Burns, K.B. Adams, and J. Longwell, J. Opt. Soc. Am. **40**, 339 (1950).

[21] A.-M. Siladie, G. Jacopin, A. Cros, N. Garro, E. Robin, D. Caliste, P. Pochet, F. Donatini, J. Pernot, and B. Daudin, Nano Lett. **19**, 8357 (2019).

[22] R. Vermeersch, E. Robin, A. Cros, G. Jacopin, B. Daudin, and J. Pernot, Appl. Phys. Lett. **119**, 262105 (2021).

[23] R. Vermeersch, G. Jacopin, B. Daudin, and J. Pernot, Appl. Phys. Lett. **120**, 162104 (2022).